

Event-based switching control for networked switched systems under nonperiodic DoS jamming attacks

ISSN 1751-8644

Received on 2nd May 2020

Revised 2nd September 2020

Accepted on 20th October 2020

E-First on 22nd January 2021

doi: 10.1049/iet-cta.2020.0536

www.ietdl.org

Fan Yang¹, Zhou Gu¹ ✉, Engang Tian², Shen Yan¹¹College of Mechanical & Electronic Engineering, Nanjing Forestry University, No. 159, Longbo Road, Nanjing, People's Republic of China²School of Optical-Electrical and Computer Engineering, University of Shanghai for Science and Technology, No.516, Jungong Road, Yangpu District, Shanghai, People's Republic of China

✉ E-mail: gzh1808@163.com

Abstract: This study addresses the event-based control of networked switched systems subject to cyber attacks. A novel mode-based event-triggered mechanism is proposed, which is capable of characterising non-periodic denial-of-service (DoS) attacks. A switching control law is employed in each subsystem to weaken the negative effects caused by DoS attacks. The time sequences of system switchings, event triggerings and intermittent DoS attack behaviours are fully investigated, which yields a resultant closed control system. Then, by using piecewise Lyapunov functional methods, sufficient conditions are formulated to guarantee the concerned system exponentially stable. Meanwhile, the co-design methods for switching controllers and event-triggering parameters can be developed. Finally, a numerical simulation example and a practical example of a second-order oscillating circuit are presented to verify the proposed methods.

1 Introduction

Switched systems have been applied in various fields due to their capacity of modelling complex or uncertain systems [1]. By importing an additional degree of freedom, switched systems contribute to realising intelligent control or adaptive control. However, more challenges are brought in due to their diverse and complex dynamics, which lead to remarkable results. To mention a few, stability problems were investigated on various categories of switching signals, in which the case of arbitrary switching is an important branch [2]. Cetinkaya *et al.* [3] mentioned that the concepts of dwell-time and average dwell-time were usually utilised to restrain the switching manners. The literature works [4, 5] were concerned with the stabilisation performance of stable or unstable subsystems. In recent years, the problem of asynchronous control has been arousing great research interests [6].

With the development of communication technologies, shared networks are used to transmit data. Switched systems are no exception to this tendency, and networked switched systems have become a hot issue at the present time [7, 8]. Although this kind of system inherits the advantages of networked control systems, a series of phenomena caused by networks can not be ignored, such as network congestions and transmission delays, which inspire plenty of outcomes [9–11] and the reference therein. For saving network resources, the concept of event-triggered control was proposed in the late 1990s [12]. By considering the digital nature of networks, Yue *et al.* [13] developed an effective event-triggered communication scheme in the continuous-time domain with inter-sampling behaviours. This kind of event-triggered mechanism (ETM) skillfully excludes the Zeno behaviour and shows its advantages when dealing with the issue of transmission delays, which is widely utilised in various fields, such as networked filtering [14, 15], networked control [16–18], and consensus problems of multiagent systems [19]. In nature, networked control systems with an event-triggered strategy are a category of hybrid systems with complex dynamic characteristics [20]. Their combination with switched systems heralds more potential and promising work and some research work has been rising from this point of view. Xiang and Johnson [21] incorporated a periodical sampling scheme and an event-triggering strategy into switched systems to analyse the asymptotic stability problem, in which switchings were only permitted at sampling instants. This

hypothesis indeed simplifies the analytic process but yields too much conservativeness. In [8, 22], network transmission delays were taken into consideration when dealing with event-triggered control problems for network-based switched linear systems. Compared to typical physical plants, [8, 23] considered the situation that the mode signal and the state signal were simultaneously transmitted to the remote controllers, and the asynchronous phenomenon between the subsystems and controllers had to be addressed. However, it conversely makes the analytic process rather complicated while the related analysis of system dynamics is not thoroughly investigated. Roughly speaking, the research on the control issue of networked switched systems is still largely open, which inspires one motivation of this study.

In addition, networked control systems are vulnerable to cyber attacks while the denial-of-service (DoS) attack is a primary branch [24, 25]. One major task of this issue is to establish appropriate mathematical models. In [26], the DoS attack was treated as a special class of network-induced delay and then conventional analysis approaches were employed. Stochastic models, such as Bernoulli models [27] and Markov models [28], were established to depict the uncertainties of DoS attacks. In contrast, [29] pointed out that it was difficult to determine the intentions of DoS attackers, and there existed many limitations for a certain kind of statistical models. A general DoS attack underlying strategy was addressed and the attack behaviours were restrained by the DoS frequency and DoS duration. On another hand, [30] mentioned that it was of practical significance to consider security requirements and resource constraints comprehensively, which arouses great interests recently and leads researchers to some preliminary results. In contrast to conventional assumptions where the synchronous DoS attacks or attacks only on one channel were considered, literature works [31, 32] addressed the event-triggered control issue under asynchronous DoS attacks. In [33], the influence of DoS attacks was treated as a kind of packet dropouts. It was characterized by a security-oriented resilient triggering strategy while the triggering time-sequence was quite puzzling. Sun and Yang [34] integrated a periodic update policy into the ETM. Although the influence of DoS attacks can be counteracted, the related time series analysis is quite complex, which may limit its further application to other systems, for instance, switched systems. The literature works [35, 36] modelled the studied system as a switched system in accordance with the course of DoS attacks,

which was appropriate to deal with both periodic or non-periodic DoS attacks. However, an open-loop control scheme was selected during the duration of DoS attacks, which resulted in some potential safety hazard to some extent. Liu *et al* [37] was concerned with the event-triggered load frequency control problem under hybrid cyber attacks, including DoS attacks and stochastic deception attacks. In [38], the secure consensus problem of multiagent systems under DoS attacks was investigated, where the attack frequency and duration were employed to constrain DoS attacks. For switched systems, there have been a few research works accounting for resource constraints and DoS attacks simultaneously in the literature, which also motivates us in present work.

Accordingly and in view of the above discussions, this work addresses the event-based control of networked switched systems subject to non-periodic DoS attacks. It is not just a simple combination of switched systems, resource constraints and cyber attacks. The major challenge lies in the complex system dynamics, that is, the interactions of event triggerings, system switchings and intermittent DoS attack behaviours. So, we devote ourselves to simplifying the system dynamics and establishing a unified analytic model, and the contributions of this paper can be highlighted as follows: (i) a mode-based ETM is proposed in accordance with the sleeping mode and the active mode of intermittent DoS attacks. To the best of our knowledge, it is a novel mathematical model to depict the influences of DoS attacks; (ii) different from the case in [35] where an open-loop control scheme is considered, this paper integrates secondary switching controllers and zero-order holder (ZOH) in the communication scheme, which makes the system under closed-loop control all the time to resist DoS attacks; (iii) through time series analysis approaches, the switched system with an event-based switching control strategy under non-periodic DoS attacks is converted to a unified resultant model; (iv) by using piecewise Lyapunov functional methods, sufficient conditions are derived to ensure the system exponentially stable (ES). Furthermore, we develop a co-design method for the controller gains and the weighting matrices in the ETM.

Notation: Throughout this paper, \mathbb{R}^m represents the m -dimensional Euclidean space, I is an identity matrix with adjustable dimensions, and $\mathbb{R}^{n \times m}$ denotes a set of $n \times m$ real matrices. For a real number c , $\lfloor c \rfloor$ means the largest integer less than or equal to c . For a matrix P , P^{-1} refers to its inverse while P^T denotes the transpose. For a symmetric matrix P , we define $\lambda_{\min}(P)$ and $\lambda_{\max}(P)$ as the minimum and maximal eigenvalue of P . Without special declarations, matrices are assumed to have compatible dimensions.

2 Preliminaries

A typical event-based communication scheme of the networked switched system is shown in Fig. 1. In the framework, the periodically sampled system state is transmitted over wireless networks, which is vulnerable to non-periodic DoS attacks. In particular, switching controllers are adopted in each subsystem and an intelligent decision unit is placed at the local actuator side, which is used to determine the exact online controller according to the current system mode. A ZOH is employed to hold the updated control information until the next event occurs, while another ZOH is employed to hold the system state. Note that the ZOHs are always in working condition, even if the system is under DoS attacks. In the following, the mathematical models of the physical plant, event trigger, switching controllers and non-periodic DoS attacks will be described in detail.

2.1 Physical plant

The concerned linear switched system is described as:

$$\dot{x}(t) = A_{\sigma(t)}x(t) + B_{\sigma(t)}u(t) \quad (1)$$

where $x(t) \in \mathbb{R}^{n_x}$ and $u(t) \in \mathbb{R}^{n_u}$ denote the state vector and control input, respectively. $\sigma(t): [0, \infty) \mapsto \mathcal{L} = \{1, 2, \dots, M\}$ represents the switching signal, which is a piecewise continuous function. To be

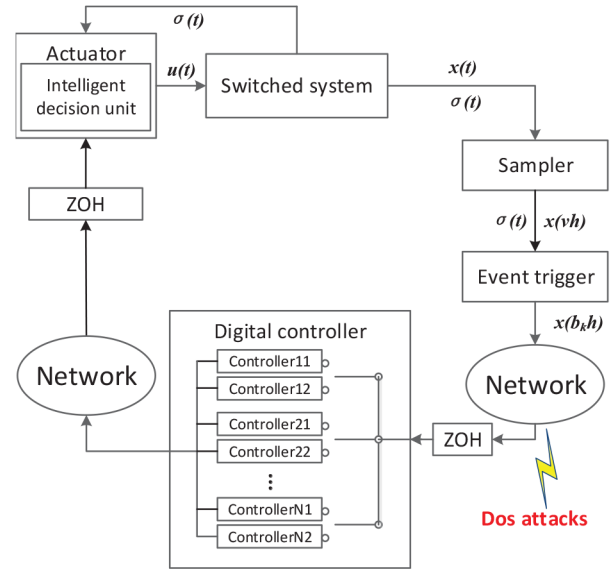


Fig. 1 System plant

specific, the switching sequences can be redefined as $\sigma(t) = \{(l_0, \sigma(l_0)), (l_1, \sigma(l_1)), \dots, (l_q, \sigma(l_q)), \dots\}$ with $l_0 = 0$. When $t \in [l_q, l_{q+1})$, we say that the system mode $\sigma(l_q)$ is online with corresponding system matrices $A_{\sigma(l_q)}$ and $B_{\sigma(l_q)}$.

Remark 1: Different from the system framework in [8], the switching mode signal is not transmitted through the network into the controllers but sent to the local actuator side. There is no necessary to use the network to execute the data exchange between the switched system and the local actuator, for instance, the serial communication mode (RS485 bus) can be adopted. Furthermore, we assume that digital controllers are employed and the control information of all sub-controllers are sent to the actuator. Then, the intelligent decision unit at the actuator side is capable of selecting the exact control information according to the active system mode. In this sense, the asynchronous phenomenon is beyond the scope of this paper.

Before proceeding further, the following assumptions are of great significance for detailed design work.

Assumption 1: The system states are fully measurable. The implementations of data sampling and transmission in the physical plant are assumed to be instant. That is, the network-induced delays, data losses and disorders are out of the scope of this paper.

Assumption 2: As mentioned in [32], the forward and backward communication channels may be attacked asynchronously. However, this issue is not the main concern of this work, and we assume only the forward channel is vulnerable to DoS attacks. Furthermore, the cyber attack is detectable.

Remark 2: As shown in Fig. 1, only the data exchanges among the event trigger, remote controllers and the local actuator are executed through networks, where the corresponding network channels are called the forward and backward communication channels, respectively. Both two channels can be attacked in practice. Except for the asynchronous issue, owing to the existence of the ZOHs, the effects of attacks on the system can be considered as the same in the following situations, only the forward channel is attacked, or only the backward channel is attacked, or the two channels are attacked synchronously.

Assumption 3: The frequency of data sampling is always higher than that of system switching.

Remark 3: With the evolution of sampling techniques, it is not difficult for the sampling frequency to reach the level of 1 kHz. Comparatively speaking, the frequency of system switching is much lower in consideration of physical constraints, for instance,

the inertia of practical systems. Hence, Assumption 3 is consistent with reality, which will greatly contribute to the analysis of system dynamics.

2.2 Modelling of DoS attacks

We consider a kind of power-constrained jamming signal [39] expressed as:

$$\Gamma(t) = \begin{cases} 1, & t \in [d^n, d^n + d_{\text{off}}^n) \\ 2, & t \in [d^n + d_{\text{off}}^n, d^{n+1}) \end{cases} \quad (2)$$

where the time sequences $\{d^n\}_{n \in \mathbb{N}}$ and $\{d^n + d_{\text{off}}^n\}_{n \in \mathbb{N}}$ denote the instants when DoS on/off and off/on transitions occur, and satisfy $d^n < d^n + d_{\text{off}}^n < d^{n+1}$ for $n \in \mathbb{N}$. From the definition above, it is indicated that the concerned system is healthy and network communications are permitted in the intervals $\bigcup_{n \in \mathbb{N}} [d^n, d^n + d_{\text{off}}^n)$ while the concerned system is suffering from jamming attacks and network communications are denied in the intervals $\bigcup_{n \in \mathbb{N}} [d^n + d_{\text{off}}^n, d^{n+1})$. Considering the power-constrained characteristic of DoS attacks and inspired by [36], we make the following assumption:

Assumption 4: For the time interval $\Lambda_{n,1} = [d^n, d^n + d_{\text{off}}^n)$, there always exists a positive scalar d_{min} satisfying

$$\inf_{n \in \mathbb{N}} \{d_{\text{off}}^n\} \geq d_{\text{min}} \quad (3)$$

where $\{\Lambda_{n,1}\}$ are called the sleeping intervals of DoS attacks.

For the time interval $\Lambda_{n,2} = [d^n + d_{\text{off}}^n, d^{n+1})$, there always exists a positive scalar d_{max} satisfying

$$\sup_{n \in \mathbb{N}} \{d_{\text{on}}^n\} \leq d_{\text{max}} \quad (4)$$

where $\{\Lambda_{n,2}\}$ are called the active intervals of DoS attacks and we define $d_{\text{on}}^n = d^{n+1} - d^n - d_{\text{off}}^n$.

Remark 4: Compared to periodic DoS attacks considered in [35], non-periodic ones are more consistent with the nature of cyber attacks and it may bring more challenges for the controller design. We define $T_{\text{DoS}}^n = d_{\text{off}}^n + d_{\text{on}}^n$ as a full attack period, then the values of $\{T_{\text{DoS}}^n\}$, $\{d_{\text{off}}^n\}$ and $\{d_{\text{on}}^n\}$ are time-varying.

Remark 5: From the jamming signal (2), it is indicated that the introduced DoS attack is intermittent, which is reasonable with respect to its power-constrained characteristic. The concepts of DoS duration and frequency [29] are more likely to reflect the distributions of DoS attacks. Comparatively speaking, Assumption 4 depicts the constraints of DoS attacks from a more micro perspective with d_{min} and d_{max} . The sleeping intervals $\{\Lambda_{n,1}\}$ and active intervals $\{\Lambda_{n,2}\}$ are considered as individual behaviours, that is, they may cause completely different effects on the system performance.

2.3 Design of event-triggered mechanism

Taking no account of the effect of DoS attacks, an ETM similar to that in [13] is introduced to improve the utilisation rate of network resources:

$$t_{k+1}h = t_k h + \min_{v \geq 1, v \in \mathbb{N}} \{vh \mid e_k^T(t)\Omega e_k(t)\} \geq \delta x^T(t_k h + vh)\Omega x(t_k h + vh) \quad (5)$$

where h is the constant sampling period, δ is a predefined scalar, $t_k h$ denotes the last triggering instant, $x(t_k h + vh)$ is the current sampled state, the state error $e_k(t) \triangleq x(t_k h) - x(t_k h + vh)$,

$v = \{1, 2, \dots, t_{k+1}h - t_k h - 1\}$, $\Omega > 0$ is a weighting matrix to be designed.

Owing to the ZOH in the physical plant, the control input of switched systems holds until next event, which is given as

$$u(t) = K_{\sigma(t)}x(t_k h), \quad t \in [t_k h, t_{k+1}h) \quad (6)$$

where the controller gain $K_{\sigma(t)}$ is corresponding to each subsystem.

Note that the transmission failure of triggered data $x(t_k h)$ caused by DoS attacks will greatly degrade the control performance. Hence, an effort should be made for the event-triggered communication scheme to be perfect and weaken the influence of non-periodic DoS attacks.

Considering the nature of DoS attacks, completely blocking network communications in the intervals $\bigcup_{n \in \mathbb{N}} [d^n + d_{\text{off}}^n, d^{n+1})$, a novel ETM can be established as:

$$b_{k+1}h = b_k h + \min_{v \geq 1, v \in \mathbb{N}} \{vh \mid e_k^T(t)\Omega_{\sigma(t), \Gamma(t)} e_k(t)\} \geq \delta_{\Gamma(t)} x^T(b_k h + vh)\Omega_{\sigma(t), \Gamma(t)} x(b_k h + vh) \quad (7)$$

where $\{b_k h\}$ denotes the triggering sequences under DoS attacks. Different from the Ω and δ in (5), $\Omega_{\sigma(t), \Gamma(t)}$ and $\delta_{\Gamma(t)}$ are related to the DoS jamming signal and the switching signal. When $\Gamma(t) = 1$, $\delta_1 \in [0, 1)$; when $\Gamma(t) = 2$, $\delta_2 \rightarrow \infty$. The definitions of other parameters can refer to the ETM (5).

Remark 6: From the definitions above, we set strict limitations on the value of $\delta_{\Gamma(t)}$. $\delta_1 \in [0, 1)$ represents that communications are allowed according to control demands while $\delta_2 \rightarrow \infty$ indicates that no events will occur, which are corresponding to the sleeping mode and the active mode of DoS attacks, respectively. In fact, the ETM (7) where $\Gamma(t) = 2$ is used to depict the influences of DoS attacks in systematic analysis and controller design. Note that only the following ETM will be executed in the physical plant, which is called an online ETM

$$b_{k+1}h = b_k h + \min_{v \geq 1, v \in \mathbb{N}} \{vh \mid e_k^T(t)\Omega_{\sigma(t), 1} e_k(t)\} \geq \delta_1 x^T(b_k h + vh)\Omega_{\sigma(t), 1} x(b_k h + vh) \quad (8)$$

2.4 Design of switching controllers

This work introduces a switching control strategy in the event-based communication scheme to resist DoS attacks. Before designing a switching control law, we first make an in-depth analysis of the time sequences of sampling instants and non-periodic DoS attacks. As shown in Fig. 2, the sleeping intervals $\{\Lambda_{n,1}\}$ and the active intervals $\{\Lambda_{n,2}\}$ are random and alternant. Based on the ETM (7), we can see that data transmissions over networks will only occur at the sampling instants $\{kh\}$. So, we can redefine the effective attack sequences based on (2):

$$\Gamma(t) = \begin{cases} 1, & t \in [D^n, D^n + D_{\text{off}}^n) \\ 2, & t \in [D^n + D_{\text{off}}^n, D^{n+1}) \end{cases} \quad (9)$$

where $D^n = (\lfloor d^n/h \rfloor + 1)h$, $D_{\text{off}}^n = (\lfloor (d^n + d_{\text{off}}^n)/h \rfloor + 1)h - D^n$, detailed explanations of parameters are similar to the ones in (2) and we omit them here.

Without loss of generality, we update Assumption 4 as follows:

Assumption 5: For the time interval $\Upsilon_{n,1} = [D^n, D^n + D_{\text{off}}^n)$, we have

$$\inf_{n \in \mathbb{N}} \{D_{\text{off}}^n\} \geq D_{\text{min}} = \lfloor d_{\text{min}}/h \rfloor h \quad (10)$$

For the time interval $\Upsilon_{n,2} = [D^n + D_{\text{off}}^n, D^{n+1})$, we have

$$\sup_{n \in \mathbb{N}} \{D_{\text{on}}^n\} \leq D_{\text{max}} = (\lfloor d_{\text{max}}/h \rfloor + 1)h \quad (11)$$

where $D_{\text{on}}^n = D^{n+1} - D^n - D_{\text{off}}^n$.

Remark 7: For instance, as shown in Fig. 2, the first active interval $\Lambda_{1,2}$ comes between the third and fourth sampling instant. Based on the ETM (7), the fourth sampling instant is the first one affected by the attack in nature. Hence, the above equivalence method dealing with non-periodic DoS attacks are reasonable, which brings great convenience to the following design work. Moreover, the case $D_{\text{off}}^n \rightarrow \infty$ denotes that the concerned system is healthy without any cyber attacks, and well control performance can be guaranteed. The case $0 \leq D_{\text{on}}^n < h$ is also out of scope of this work because this kind of DoS attacks has no effect on the communication scheme.

Combining the state feedback controller (6), we give the switching control law as follows:

$$u(t) = K_{\sigma(t), \Gamma(t)} x(b_k h), \quad t \in [b_k h, b_{k+1} h) \quad (12)$$

Remark 8: Unlike the design in [36] that the control loop is open over $\{\Lambda_{n,2}\}$, secondary sub-controllers need to be designed for every subsystem in this work. That is, if the switched system is consist of N subsystems, then $2N$ sub-controllers are at service. Moreover, from the view of physical implementation, an intelligent decision unit in Fig. 1 is utilised to execute the switching control law according to detected attack modes and local sampling sequences. That is, switchings of sub-controllers are only executed at the sampling instants if a change of attack modes has been detected, which is consistent with the equivalent processing of DoS attacks illustrated in Remark 7.

2.5 Co-design of switching controllers and ETM

Based on the ETM (7) and the switching control law (12), a unified resultant model of the concerned system will be formulated. Inspired by [13], we divide the event triggering interval $\zeta_k \triangleq [b_k h, b_{k+1} h)$ into sampling interval-like subintervals $\chi_{k,v}^{\Gamma(t)} \triangleq [S_{k,v}^{\Gamma(t)}, S_{k,v+1}^{\Gamma(t)})$, where $S_{k,v}^{\Gamma(t)} \triangleq b_k h + v h$, $[S_{k,v}^1, S_{k,v+1}^1) \in \bigcup_{n \in \mathbb{N}} \Upsilon_{n,1}$ and $[S_{k,v}^2, S_{k,v+1}^2) \in \bigcup_{n \in \mathbb{N}} \Upsilon_{n,2}$. Then, it is not difficult to deduce that we can always find a scalar $v_M \in \mathbb{N}$ guaranteeing $\zeta_k = \bigcup_{v=0}^{v_M} \chi_{k,v}^{\Gamma(t)}$.

For $t \in [S_{k,v}^{\Gamma(t)}, S_{k,v+1}^{\Gamma(t)})$, defining $\eta(t) = t - b_k h - v h$ yields :

$$0 \leq \eta(t) < h \quad (13)$$

Considering $e_k(t)$, $\eta(t)$ and (12) yields that

$$u(t) = K_{\sigma(t), \Gamma(t)} x(t - \eta(t)) + e_k(t), \quad t \in \chi_{k,v}^{\Gamma(t)} \quad (14)$$

According to Assumption 3, it can be inferred that at most one switching is permitted in the interval $[S_{k,v}^{\Gamma(t)}, S_{k,v+1}^{\Gamma(t)})$, to be more specific, no switching or one switching, which is corresponding to the following two cases of the resultant system.

Case 1: Within $[S_{k,v}^{\Gamma(t)}, S_{k,v+1}^{\Gamma(t)})$, no system switching happens and the resultant system can be described as

$$\begin{cases} \dot{x}(t) = A_{\sigma(t)} x(t) + B_{\sigma(t)} K_{\sigma(t), \Gamma(t)} (x(t - \eta(t)) \\ \quad + e_k(t)), & t \in [S_{k,v}^{\Gamma(t)}, S_{k,v+1}^{\Gamma(t)}) \\ x(t) = \psi(t), & t \in [-h, 0] \end{cases} \quad (15)$$

where we supplement the initial condition of the system state $x(t)$ with a continuous function $\psi(t)$.

Case 2: Within $[S_{k,v}^{\Gamma(t)}, S_{k,v+1}^{\Gamma(t)})$, one and only switching occurs with $l_{q-1} < S_{k,v}^{\Gamma(t)} \leq l_q < S_{k,v+1}^{\Gamma(t)}$, where $\sigma(l_q) \in \mathcal{L}$. We have

$$\begin{cases} \dot{x}(t) = A_{\sigma(l_{q-1})} x(t) + B_{\sigma(l_{q-1})} K_{\sigma(l_{q-1}), \Gamma(t)} \\ \quad (x(t - \eta(t)) + e_k(t)), & t \in [S_{k,v}^{\Gamma(t)}, l_q) \\ \dot{x}(t) = A_{\sigma(l_q)} x(t) + B_{\sigma(l_q)} K_{\sigma(l_q), \Gamma(t)} \\ \quad (x(t - \eta(t)) + e_k(t)), & t \in [l_q, S_{k,v+1}^{\Gamma(t)}) \\ x(t) = \psi(t), & t \in [-h, 0] \end{cases} \quad (16)$$

Before proceeding further, the following definitions are introduced.

Definition 1: For a given switching signal $\sigma(t)$, if there exist a constant $\tau_a > 0$ and a number $N_0 > 0$ such that $N_{\sigma(t)}(t_1, t_2) \leq N_0 + (t_2 - t_1)/\tau_a$, where $0 \leq t_1 \leq t_2$, $N_{\sigma(t)}(t_1, t_2)$ denotes the switching number over (t_1, t_2) , we say $\sigma(t)$ has an average dwell time τ_a ([8], Average dwell time).

Definition 2: Let $n(T_1, T_2)$ denote the number of DoS off/on transitions over (T_1, T_2) , to be more specific, $n(T_1, T_2) = \text{card}\{n \in \mathbb{N} \mid T_1 < D^n + D_{\text{off}}^n < T_2\}$, where card represents the number of the elements in the set. If there exist a constant $\tau_b \in \mathbb{R}_{>0}$ and a number $\nu \in \mathbb{R}_{\geq 0}$ satisfying $n(T_1, T_2) \leq \nu + (T_2 - T_1)/\tau_b$ for all $T_1, T_2 \in \mathbb{R}_{\geq 0}$ with $T_1 \leq T_2$, we say that a given sequence of DoS attacks $\Upsilon_{n,2}$ satisfies the DoS frequency constraint described by τ_b and ν ([29], DoS frequency).

Definition 3 ([Exponentially stable]): The resultant system (15) and (16) is guaranteed ES, if there exist positive constants ρ and ϵ such that $\|x(t)\| \leq \epsilon e^{-\rho t} \|\psi_0\|_h$ holds for all $t > 0$, where $\|\psi_0\|_h \triangleq \sup_{-h \leq \theta \leq 0} \{ \|x(\theta)\|, \|\dot{x}(\theta)\| \}$, ρ is called the decay rate.

Based on the mode-based ETM (7), the control objective of this paper is to design suitable switching controllers for each subsystem such that the resultant system (15) and (16) is ES in the presence of the non-periodic DoS attack (9), which satisfies the power constraint in Assumption 5 and the DoS frequency constraint in Definition 2.

3 Main results

In this section, by using piecewise Lyapunov functional methods, sufficient conditions will be developed for ensuring the concerned system ES, and the controller gains are to be designed.

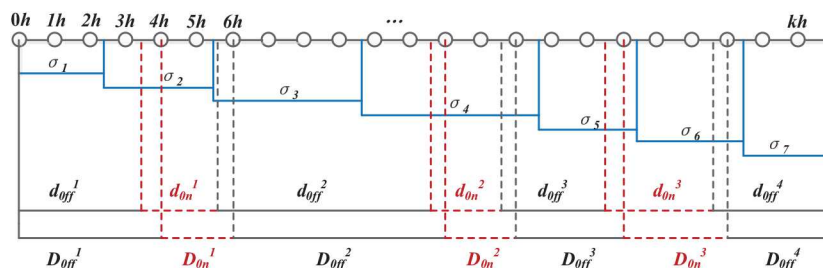


Fig. 2 Time sequence under non-periodic DoS attacks

Theorem 1: For prescribed positive scalars δ_m ($m \in \{1, 2\}$), $\delta_1 \in (0, 1)$, $\delta_2 \rightarrow \infty$, $\alpha_m, \mu_m \in (1, \infty)$, $\vartheta \in (1, \infty)$, $d_{\min}, d_{\max}, \tau_a, \tau_b, h$ and matrices K_{im} , the switched system described by (15) and (16) is ES with the proposed ETM (7) in the presence of the non-periodic DoS attack (9), if there exist positive definite matrices $P_{im} \in \mathbb{R}^{n_x \times n_x}$, $Q_{im} \in \mathbb{R}^{n_x \times n_x}$, $R_{im} \in \mathbb{R}^{n_x \times n_x}$, $Z_{im} \in \mathbb{R}^{n_x \times n_x}$, $\Omega_{im} \in \mathbb{R}^{n_x \times n_x}$, and $N_{iml}, M_{iml}, S_{iml}$ with appropriate dimensions such that $\forall (i, j) \in \mathcal{L} \times \mathcal{L}, i \neq j, l \in \{1, 2\}$

$$\varrho = -\ln \vartheta / \tau_a + (2\alpha_1 D_{\min} - 2(\alpha_1 + \alpha_2)h - 2\alpha_2 D_{\max} - \ln(\mu_1 \mu_2)) / \tau_b > 0 \quad (17)$$

$$\Pi_1 = \begin{bmatrix} \Pi_{11} & * & * \\ \Pi_{21} & \Pi_{22} & * \\ \Pi_{31} & 0 & \Pi_{33} \end{bmatrix} < 0, \quad (18)$$

$$\begin{cases} P_{i1} \leq \mu_2 P_{i2}, P_{i2} \leq \beta \mu_1 P_{i1} \\ Q_{i1} \leq \mu_2 Q_{i2}, Q_{i2} \leq \mu_1 Q_{i1} \\ R_{i1} \leq \mu_2 R_{i2}, R_{i2} \leq \mu_1 R_{i1} \\ Z_{i1} \leq \mu_2 Z_{i2}, Z_{i2} \leq \mu_1 Z_{i1} \end{cases} \quad (19)$$

$$\begin{cases} P_{im} \leq \vartheta P_{jm} \\ Q_{im} \leq \vartheta Q_{jm} \\ R_{im} \leq \vartheta R_{jm} \\ Z_{im} \leq \vartheta Z_{jm} \end{cases} \quad (20)$$

where

$$\begin{aligned} \Pi_{11} &= \begin{bmatrix} \Xi_1 & * & * & * \\ \Xi_2 & \Xi_3 & * & * \\ K_{im}^T B_i^T P_{im} & 0 & -\Omega_{im} & * \\ \Xi_4 & \Xi_5 & 0 & \Xi_6 \end{bmatrix}, \\ \Pi_{21} &= \begin{bmatrix} \sqrt{h} A_i & 0 & \sqrt{h} B_i K_{im} & \sqrt{h} B_i K_{im} \\ \sqrt{h} A_i & 0 & \sqrt{h} B_i K_{im} & \sqrt{h} B_i K_{im} \end{bmatrix}, \\ \Pi_{22} &= \text{diag}\{-R_{im}^{-1}, -Z_{im}^{-1}\}, \\ \Pi_{31} &= \begin{bmatrix} \sqrt{h} M_{im1}^T & \sqrt{h} M_{im2}^T & 0 & 0 \\ \sqrt{h} N_{im1}^T & 0 & 0 & \sqrt{h} N_{im2}^T \\ 0 & \sqrt{h} S_{im1}^T & 0 & \sqrt{h} S_{im2}^T \end{bmatrix}, \\ \Pi_{33} &= \text{diag}\{-e^{-2(2-m)\alpha_m h} Z_{im}, -e^{-2(2-m)\alpha_m h} R_{im}, \\ &\quad -e^{-2(2-m)\alpha_m h} R_{im}\}, \\ \Xi_1 &= (-1)^{m-1} 2\alpha_m P_{im} + A_i^T P_{im} + P_{im} A_i + Q_{im} \\ &\quad + M_{im1} + M_{im1}^T + N_{im1} + N_{im1}^T, \\ \Xi_2 &= -M_{im1}^T + M_{im2}, \beta = e^{2(\alpha_1 + \alpha_2)h}, \\ \Xi_3 &= -e^{(-1)^{m-1} 2\alpha_m h} Q_{im} - M_{im2} - M_{im2}^T - S_{im1} - S_{im1}^T, \\ \Xi_4 &= K_{im}^T B_i^T P_{im} - N_{im1}^T + N_{im2}, \Xi_5 = -S_{im1}^T - S_{im2}, \\ \Xi_6 &= -N_{im2} - N_{im2}^T + S_{im2} + S_{im2}^T + \delta_m \Omega_{im}, \\ D_{\min} &= \lfloor d_{\min} / h \rfloor h, D_{\max} = (\lfloor d_{\max} / h \rfloor + 1)h. \end{aligned}$$

Proof: Consider the following Lyapunov functional candidate:

$$\begin{aligned} V_{\sigma(t), \Gamma(t)}(t) &= x^T(t) P_{\sigma(t), \Gamma(t)} x(t) \\ &\quad + \int_{t-h}^t \kappa_{\Gamma(t)} x^T(s) Q_{\sigma(t), \Gamma(t)} x(s) ds \\ &\quad + \int_{-h}^0 \int_{t+v}^t \kappa_{\Gamma(t)} \dot{x}^T(s) R_{\sigma(t), \Gamma(t)} \dot{x}(s) ds dv \\ &\quad + \int_{-h}^0 \int_{t+v}^t \kappa_{\Gamma(t)} \dot{x}^T(s) Z_{\sigma(t), \Gamma(t)} \dot{x}(s) ds dv \end{aligned} \quad (21)$$

where $P_{\sigma(t), \Gamma(t)}$, $Q_{\sigma(t), \Gamma(t)}$, $R_{\sigma(t), \Gamma(t)}$, and $Z_{\sigma(t), \Gamma(t)}$ are positive definite matrices, $\kappa_{\Gamma(t)} \triangleq e^{2(-1)^{\Gamma(t)} \alpha_{\Gamma(t)}(t-s)}$, and $\alpha_{\Gamma(t)}$ is a positive scalar.

Case 1: Consider the system (15). For $t \in [S_{k,v}^{\Gamma(t)}, S_{k,v+1}^{\Gamma(t)})$, no system switching occurs. The switching mode $i \in \mathcal{L}$ is assumed to be active and let $m = \Gamma(t) \in \{1, 2\}$.

First, we consider the situation that $[S_{k,v}^m, S_{k,v+1}^m) \in \bigcup_{n \in \mathbb{N}} \Upsilon_{n,1}$ with $m = 1$. The time derivative of $V_{i1}(t)$ is

$$\begin{aligned} \dot{V}_{i1}(t) &= -2\alpha_1 V_{i1}(t) + x^T(t) (2\alpha_1 P_{i1} + A_i^T P_{i1} \\ &\quad + P_{i1} A_i + Q_{i1}) x(t) \\ &\quad + 2x(t - \eta(t))^T K_{i1}^T B_i^T P_{i1} x(t) \\ &\quad + 2e_{\kappa}(t)^T K_{i1}^T B_i^T P_{i1} x(t) \\ &\quad + h \dot{x}^T(t) R_{i1} \dot{x}(t) + h \dot{x}^T(t) Z_{i1} \dot{x}(t) \\ &\quad - e^{-2\alpha_1 h} x(t-h)^T Q_{i1} x(t-h) \\ &\quad + e_{\kappa}^T(t) \Omega_{i1} e_{\kappa}(t) - e_{\kappa}^T(t) \Omega_{i1} e_{\kappa}(t) \\ &\quad - \int_{t-h}^t e^{-2\alpha_1(t-s)} \dot{x}(s)^T Z_{i1} \dot{x}(s) ds \\ &\quad - \int_{t-h}^{t-\eta(t)} e^{-2\alpha_1(t-s)} \dot{x}(s)^T R_{i1} \dot{x}(s) ds \\ &\quad - \int_{t-\eta(t)}^t e^{-2\alpha_1(t-s)} \dot{x}(s)^T R_{i1} \dot{x}(s) ds \\ &\quad + 2\xi^T(t) M_{i1} G_1(t) + 2\xi^T(t) N_{i1} G_2(t) \\ &\quad + 2\xi^T(t) S_{i1} G_3(t) \end{aligned} \quad (22)$$

where

$$\begin{aligned} \xi(t) &= [x^T(t) \quad x^T(t-h) \quad e_{\kappa}^T(t) \quad x^T(t-\eta(t))]^T, \\ M_{i1} &= [M_{i11}^T \quad M_{i12}^T \quad 0 \quad 0]^T, \\ N_{i1} &= [N_{i11}^T \quad 0 \quad 0 \quad N_{i12}^T]^T, \\ S_{i1} &= [0 \quad S_{i11}^T \quad 0 \quad S_{i12}^T]^T, \\ G_1(t) &= x(t) - x(t-h) - \int_{t-h}^t \dot{x}(s) ds, \\ G_2(t) &= x(t) - x(t-\eta(t)) - \int_{t-\eta(t)}^t \dot{x}(s) ds, \\ G_3(t) &= x(t-\eta(t)) - x(t-h) - \int_{t-h}^{t-\eta(t)} \dot{x}(s) ds. \end{aligned}$$

For matrices $M_{i1}, N_{i1}, S_{i1}, R_{i1} > 0$ and $Z_{i1} > 0$, it is clear that

$$-2\xi^T(t) M_{i1} \int_{t-h}^t \dot{x}(s) ds \leq h \xi^T(t) M_{i1} e^{2\alpha_1 h} Z_{i1}^{-1} M_{i1}^T \xi(t) + \int_{t-h}^t e^{-2\alpha_1 h} \dot{x}(s) Z_{i1} \dot{x}(s) ds \quad (23)$$

$$-2\xi^T(t) N_{i1} \int_{t-\eta(t)}^t \dot{x}(s) ds \leq h \xi^T(t) N_{i1} e^{2\alpha_1 h} R_{i1}^{-1} N_{i1}^T \xi(t) + \int_{t-\eta(t)}^t e^{-2\alpha_1 h} \dot{x}(s) R_{i1} \dot{x}(s) ds \quad (24)$$

$$-2\xi^T(t) S_{i1} \int_{t-h}^{t-\eta(t)} \dot{x}(s) ds \leq h \xi^T(t) S_{i1} e^{2\alpha_1 h} R_{i1}^{-1} S_{i1}^T \xi(t) + \int_{t-h}^{t-\eta(t)} e^{-2\alpha_1 h} \dot{x}(s) R_{i1} \dot{x}(s) ds \quad (25)$$

Meanwhile, we notice that

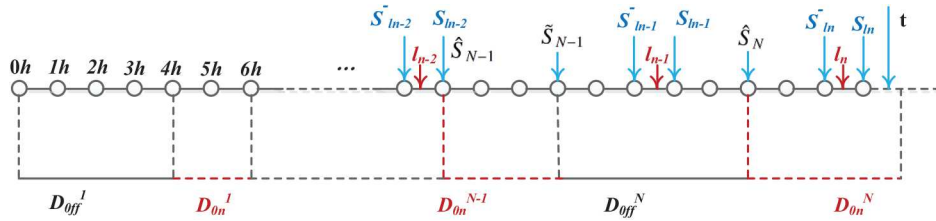


Fig. 3 Time sequence under non-periodic DoS attacks

$$\begin{aligned}
 & - \int_{t-h}^t e^{-2\alpha_1(t-s)} \dot{x}(s)^T Z_{i1} \dot{x}(s) ds \\
 & \leq - \int_{t-h}^t e^{-2\alpha_1 h} \dot{x}(s)^T Z_{i1} \dot{x}(s) ds
 \end{aligned} \tag{26}$$

$$V(t) \leq \begin{cases} e^{-2\alpha_1(t-S_{k,v}^1)} V_{i1}(S_{k,v}^1), & t \in [S_{k,v}^1, S_{k,v+1}^1) \\ e^{2\alpha_2(t-S_{k,v+1}^2)} V_{i2}(S_{k,v+1}^2), & t \in [S_{k,v+1}^2, S_{k,v+2}^2) \end{cases} \tag{35}$$

$$\begin{aligned}
 & - \int_{t-h}^{t-\eta(t)} e^{-2\alpha_1(t-s)} \dot{x}(s)^T R_{i1} \dot{x}(s) ds \\
 & \leq - \int_{t-h}^{t-\eta(t)} e^{-2\alpha_1 h} \dot{x}(s)^T R_{i1} \dot{x}(s) ds
 \end{aligned} \tag{27}$$

$$\begin{aligned}
 & - \int_{t-\eta(t)}^t e^{-2\alpha_1(t-s)} \dot{x}(s)^T R_{i1} \dot{x}(s) ds \\
 & \leq - \int_{t-\eta(t)}^t e^{-2\alpha_1 h} \dot{x}(s)^T R_{i1} \dot{x}(s) ds
 \end{aligned} \tag{28}$$

Combining the triggering condition in (7) and (22)–(28), we have

$$\begin{aligned}
 \dot{V}_{i1}(t) & \leq -2\alpha_1 V_{i1}(t) + \xi^T(t) (\Pi_{i1} - \Pi_{21}^T \Pi_{22}^{-1} \Pi_{21} \\
 & + h M_{i1} e^{2\alpha_1 h} Z_{i1}^{-1} M_{i1}^T + h N_{i1} e^{2\alpha_1 h} R_{i1}^{-1} N_{i1}^T \\
 & + h S_{i1} e^{2\alpha_1 h} R_{i1}^{-1} S_{i1}^T) \xi(t)
 \end{aligned} \tag{29}$$

By using the Schur's complement and the sufficient condition (18), it can be derived that

$$\dot{V}_{i1}(t) \leq -2\alpha_1 V_{i1}(t), \quad t \in [S_{k,v}^1, S_{k,v+1}^1) \tag{30}$$

Integrating both sides of (30), we have

$$V_{i1}(t) \leq e^{-2\alpha_1(t-S_{k,v}^1)} V_{i1}(S_{k,v}^1), \quad t \in [S_{k,v}^1, S_{k,v+1}^1) \tag{31}$$

Next, a similar analysis process is conducted for $[S_{k,v}^m, S_{k,v+1}^m) \in \bigcup_{n \in \mathbb{Z}} \Upsilon_{n,2}$ with $m = 2$. It can be deduced that

$$\begin{aligned}
 \dot{V}_{i2}(t) & \leq 2\alpha_2 V_{i2}(t) + \xi^T(t) (\Pi_{i1} - \Pi_{21}^T \Pi_{22}^{-1} \Pi_{21} \\
 & + h M_{i2} Z_{i2}^{-1} M_{i2}^T + h N_{i2} R_{i2}^{-1} N_{i2}^T \\
 & + h S_{i2} R_{i2}^{-1} S_{i2}^T) \xi(t)
 \end{aligned} \tag{32}$$

Similarly, considering the sufficient condition (18) yields

$$V_{i2}(t) \leq e^{2\alpha_2(t-S_{k,v}^2)} V_{i2}(S_{k,v}^2), \quad t \in [S_{k,v}^2, S_{k,v+1}^2) \tag{33}$$

Then, for $m \in \{1, 2\}$, a unified preliminary conclusion is given as follows

$$V_{im}(t) \leq e^{2(-1)^m \alpha_m(t-S_{k,v}^m)} V_{im}(S_{k,v}^m), \quad t \in [S_{k,v}^m, S_{k,v+1}^m) \tag{34}$$

We assume that $[S_{k,v}^1, S_{k,v+1}^1)$ and $[S_{k,v+1}^2, S_{k,v+2}^2)$ are two adjacent sampling intervals under different attack modes. According to (34), we have

Taking the sufficient condition (19) into account, it is easy to show that

$$V_{i2}(S_{k,v+1}^2) \leq \beta \mu_1 V_{i1}(S_{k,v+1}^1) \tag{36}$$

Similarly, we assume that $[S_{k,v}^2, S_{k,v+1}^2)$ and $[S_{k,v+1}^1, S_{k,v+2}^1)$ are two adjacent sampling intervals under different attack modes. It can be deduced that

$$V_{i1}(S_{k,v+1}^1) \leq \mu_2 V_{i2}(S_{k,v+1}^2) \tag{37}$$

Case 2: Consider the system (16). As there exists only one switching in the interval $[S_{k,v}^m, S_{k,v+1}^m)$, we assume $l_i < S_{k,v}^m \leq l_j < S_{k,v+1}^m$, where $(i, j) \in \mathcal{L} \times \mathcal{L}, i \neq j$, that is, the subsystem i is active for $t \in [S_{k,v}^m, l_j)$ and the subsystem j is active for $t \in [l_j, S_{k,v+1}^m)$.

For $t \in [S_{k,v}^m, l_j)$, similar to the analysis process in Case 1, one has

$$V_{im}(t) \leq e^{2(-1)^m \alpha_m(t-S_{k,v}^m)} V_{im}(S_{k,v}^m) \tag{38}$$

For $t \in [l_j, S_{k,v+1}^m)$, according to the sufficient condition (20), we have

$$V_{jm}(t) \leq \vartheta V_{im}(t) \leq \vartheta e^{2(-1)^m \alpha_m(t-S_{k,v}^m)} V_{im}(S_{k,v}^m) \tag{39}$$

Next, we try to give a general conclusion on $V(t)$ for $t > 0$ by combining Cases 1 and 2. Before proceeding further, some symbols should be predefined. Let n be the switching number of $\sigma(t)$ over $(0, t)$ with the corresponding switching instants $\{l_1, l_2, \dots, l_n\}$, let N denote the number of DoS off/on transitions over $(0, t)$, and let S_{in}^- and S_{in}^+ be the sampling instants right before and after l_n , respectively, which yields $l_n \in [S_{in}^-, S_{in}^+)$. Meanwhile, we define \hat{S}_N as the corresponding sampling instant when the N th DoS off/on transition occurs, and let \tilde{S}_N be the corresponding sampling instant when the N th DoS on/off transition occurs.

As the instants of system switchings and non-periodic DoS attacks are intertwined and irregular, a random example is illustrated in Fig. 3, in which we consider the first situation $t \in \bigcup_{n \in \mathbb{N}} \Upsilon_{n,1}$.

Combining (34)–(39) and Assumption 5 yields that

$$\begin{aligned}
 V(t) &\leq e^{2\alpha_2(t-S_{l_n})} V_{\sigma(l_n), 2}(S_{l_n}) \\
 &\leq \vartheta e^{2\alpha_2(t-S_{l_n}^-)} V_{\sigma(l_n-1), 2}(S_{l_n}^-) \\
 &\leq \vartheta e^{2\alpha_2(t-\hat{S}_N)} V_{\sigma(l_n-1), 2}(\hat{S}_N) \\
 &\leq \vartheta \beta \mu_1 e^{2\alpha_2(t-\hat{S}_N)} V_{\sigma(l_n-1), 1}(\hat{S}_N^-) \\
 &\leq \vartheta \beta \mu_1 e^{2\alpha_2(t-\hat{S}_N)} e^{-2\alpha_1(\hat{S}_N-S_{l_n-1})} V_{\sigma(l_n-1), 1}(S_{l_n-1}) \\
 &\leq \vartheta^2 \beta \mu_1 e^{2\alpha_2(t-\hat{S}_N)} e^{-2\alpha_1(\hat{S}_N-S_{l_n-1}^-)} V_{\sigma(l_n-2), 1}(S_{l_n-1}^-) \\
 &\leq \vartheta^2 \beta \mu_1 e^{2\alpha_2(t-\hat{S}_N)} e^{-2\alpha_1(\hat{S}_N-S_{l_n-1}^-)} V_{\sigma(l_n-2), 1}(\tilde{S}_{N-1}) \\
 &\leq \vartheta^2 \beta \mu_1 \mu_2 e^{2\alpha_2(t-\hat{S}_N)} e^{-2\alpha_1(\hat{S}_N-S_{l_n-1}^-)} V_{\sigma(l_n-2), 2}(\tilde{S}_{N-1}) \\
 &\leq \vartheta^2 \beta \mu_1 \mu_2 e^{2\alpha_2 D_{\max}} e^{-2\alpha_1 D_{\min}} V_{\sigma(l_n-2), 2}(\tilde{S}_{N-1}) \\
 &\vdots \\
 &\leq \vartheta^n \beta^N \mu_1^N \mu_2^{N-1} e^{2N\alpha_2 D_{\max}} e^{-2N\alpha_1 D_{\min}} V_{\sigma(0), 1}(0) \\
 &\leq \vartheta^n \beta^N \mu_1^N \mu_2^N e^{2N\alpha_2 D_{\max}} e^{-2N\alpha_1 D_{\min}} V_{\sigma(0), 1}(0) \\
 &\leq e^{-\varrho t} V_{\sigma(0), 1}(0)
 \end{aligned} \tag{40}$$

Next, we consider another situation, $t \in \bigcup_{n \in \mathbb{N}} \Upsilon_{n,2}$, similarly, we have

$$\begin{aligned}
 V(t) &\leq \vartheta^n \beta^N \mu_1^N \mu_2^N e^{2N\alpha_2 D_{\max}} e^{-2(N+1)\alpha_1 D_{\min}} V_{\sigma(0), 1}(0) \\
 &\leq e^{-\varrho t} e^{-2\alpha_1 D_{\min}} V_{\sigma(0), 1}(0) \\
 &\leq e^{-\varrho t} V_{\sigma(0), 1}(0)
 \end{aligned} \tag{41}$$

Considering the definition of (21), one has

$$\begin{aligned}
 \Lambda_1 \|x(t)\|^2 &\leq V(0) \\
 &\leq (\lambda_2 + h\lambda_3 + (h^2/2)(\lambda_4 + \lambda_5)) \|\psi_0\|_h^2
 \end{aligned} \tag{42}$$

where $\lambda_1 = \lambda_{\min}(P_{im})$, $\lambda_2 = \lambda_{\max}(P_{im})$, $\lambda_3 = \lambda_{\max}(Q_{im})$, $\lambda_4 = \lambda_{\max}(R_{im})$ and $\lambda_5 = \lambda_{\max}(Z_{im})$.

Combining (40), (41) and (42), we have

$$\begin{aligned}
 \|x(t)\| &\leq \sqrt{\frac{\lambda_2 + h\lambda_3 + (h^2/2)(\lambda_4 + \lambda_5)}{\lambda_1}} e^{-\varrho t/2} \|\psi_0\|_h
 \end{aligned} \tag{43}$$

Hence, it implies that the concerned system is ES with a decay rate $\rho = \varrho/2$. This completes the proof. \square

Next, based on Theorem 1, the design method of switching controllers will be presented in Theorem 2.

Theorem 2: For prescribed positive scalars δ_m ($m \in \{1, 2\}$), $\delta_1 \in (0, 1)$, $\delta_2 \rightarrow \infty$, $\alpha_m, \mu_m \in (1, \infty)$, $\vartheta \in (1, \infty)$, d_{\min} , d_{\max} , $\tau_a, \tau_b, \rho_{iml}$ and h satisfying (17), the switched system described by (15) and (16) with the switching controller gains $K_{im} = Y_{im} X_{im}^{-1}$ is ES in the presence of the non-periodic DoS attack (9), if there exist positive definite matrices $X_{im} \in \mathbb{R}^{n_x \times n_x}$, $\tilde{Q}_{im} \in \mathbb{R}^{n_x \times n_x}$, $\tilde{R}_{im} \in \mathbb{R}^{n_x \times n_x}$, $\tilde{Z}_{im} \in \mathbb{R}^{n_x \times n_x}$, $\tilde{\Omega}_{im} \in \mathbb{R}^{n_x \times n_x}$ and $\tilde{N}_{iml}, \tilde{M}_{iml}, \tilde{S}_{iml}, Y_{im}$ with appropriate dimensions such that $\forall (i, j) \in \mathcal{L} \times \mathcal{L}, i \neq j, l \in \{1, 2\}$

$$\tilde{\Pi}_1 = \begin{bmatrix} \tilde{\Pi}_{11} & * & * \\ \tilde{\Pi}_{21} & \tilde{\Pi}_{22} & * \\ \tilde{\Pi}_{31} & 0 & \tilde{\Pi}_{33} \end{bmatrix} < 0, \tag{44}$$

$$\begin{cases} X_{i1} \leq \beta \mu_1 X_{i2}, X_{i2} \leq \mu_2 X_{i1}, \\ \tilde{Q}_{i1} \leq \mu_2 \tilde{Q}_{i2}, \tilde{Q}_{i2} \leq \mu_1 \tilde{Q}_{i1}, \\ \tilde{R}_{i1} \leq \mu_2 \tilde{R}_{i2}, \tilde{R}_{i2} \leq \mu_1 \tilde{R}_{i1}, \\ \tilde{Z}_{i1} \leq \mu_2 \tilde{Z}_{i2}, \tilde{Z}_{i2} \leq \mu_1 \tilde{Z}_{i1} \end{cases} \tag{45}$$

where

$$\tilde{\Pi}_{11} = \begin{bmatrix} \tilde{\Xi}_1 & * & * & * \\ \tilde{\Xi}_2 & \tilde{\Xi}_3 & * & * \\ Y_{im}^T B_i^T & 0 & -\tilde{\Omega}_{im} & * \\ \tilde{\Xi}_4 & \tilde{\Xi}_5 & 0 & \tilde{\Xi}_6 \end{bmatrix},$$

$$\tilde{\Pi}_{21} = \begin{bmatrix} \sqrt{h} A_i X_{im} & 0 & \sqrt{h} B_i Y_{im} & \sqrt{h} B_i Y_{im} \\ \sqrt{h} A_i X_{im} & 0 & \sqrt{h} B_i Y_{im} & \sqrt{h} B_i Y_{im} \end{bmatrix},$$

$$\tilde{\Pi}_{22} = \text{diag} \{ -2\rho_{im1} X_{im} + \rho_{im1}^2 \tilde{R}_{im}, -2\rho_{im2} X_{im} + \rho_{im2}^2 \tilde{Z}_{im} \},$$

$$\tilde{\Pi}_{31} = \begin{bmatrix} \sqrt{h} \tilde{M}_{im1}^T & \sqrt{h} \tilde{M}_{im2}^T & 0 & 0 \\ \sqrt{h} \tilde{N}_{im1}^T & 0 & 0 & \sqrt{h} \tilde{N}_{im2}^T \\ 0 & \sqrt{h} \tilde{S}_{im1}^T & 0 & \sqrt{h} \tilde{S}_{im2}^T \end{bmatrix},$$

$$\tilde{\Pi}_{33} = \text{diag} \{ -e^{-2(2-m)\alpha_m h} \tilde{Z}_{im}, -e^{-2(2-m)\alpha_m h} \tilde{R}_{im}, -e^{-2(2-m)\alpha_m h} \tilde{R}_{im} \},$$

$$\tilde{\Xi}_1 = (-1)^{m-1} 2\alpha_m X_{im} + X_{im} A_i^T + A_i X_{im} + \tilde{Q}_{im} + \tilde{M}_{im1} + \tilde{M}_{im1}^T + \tilde{N}_{im1} + \tilde{N}_{im1}^T,$$

$$\tilde{\Xi}_2 = -\tilde{M}_{im1} + \tilde{M}_{im2}, \beta = e^{2(\alpha_1 + \alpha_2)h},$$

$$\tilde{\Xi}_3 = -e^{-(1)^m 2\alpha_m h} \tilde{Q}_{im} - \tilde{M}_{im2} - \tilde{M}_{im2}^T - \tilde{S}_{im1} - \tilde{S}_{im1}^T,$$

$$\tilde{\Xi}_4 = Y_{im}^T B_i^T - \tilde{N}_{im1} + \tilde{N}_{im2}, \tilde{\Xi}_5 = -\tilde{S}_{im1}^T - \tilde{S}_{im2},$$

$$\tilde{\Xi}_6 = -\tilde{N}_{im2} - \tilde{N}_{im2}^T + \tilde{S}_{im2} + \tilde{S}_{im2}^T + \delta_m \tilde{\Omega}_{im},$$

$$D_{\min} = \lfloor d_{\min}/h \rfloor h, D_{\max} = (\lfloor d_{\max}/h \rfloor + 1)h.$$

Proof: According to Theorem 1, we first define $X_{im} = P_{im}^{-1}$, $\tilde{Q}_{im} = X_{im} Q_{im} X_{im}$, $\tilde{R}_{im} = X_{im} R_{im} X_{im}$, $\tilde{Z}_{im} = X_{im} Z_{im} X_{im}$, $\tilde{\Omega}_{im} = X_{im} \Omega_{im} X_{im}$, $\tilde{M}_{iml} = X_{im} M_{iml} X_{im}$, $\tilde{N}_{iml} = X_{im} N_{iml} X_{im}$, $\tilde{S}_{iml} = X_{im} S_{iml} X_{im}$, and $Y_{im} = K_{im} X_{im}$, where $m \in \{1, 2\}$, $l \in \{1, 2\}$ and $(i, j) \in \mathcal{L} \times \mathcal{L}, i \neq j$. Let $\Phi_1 = \text{diag} \{I, I, I, I, P_{im}, P_{im}, I, I, I\}$ and $\Phi_2 = \text{diag} \{X_{im}, X_{im}, X_{im}, X_{im}, X_{im}, X_{im}, X_{im}, X_{im}, X_{im}\}$.

It is not difficult to find that

$$(\rho_{im1} R_{im} - X_{im}) R_{im}^{-1} (\rho_{im1} R_{im} - X_{im}) \geq 0$$

holds for $X_{im} > 0, R_{im} > 0$ and $\rho_{im1} > 0$, which is equivalent to

$$-X_{im} R_{im}^{-1} X_{im} \leq -2\rho_{im1} X_{im} + \rho_{im1}^2 R_{im} \tag{47}$$

Similarly, we have

$$-X_{im} Z_{im}^{-1} X_{im} \leq -2\rho_{im2} X_{im} + \rho_{im2}^2 Z_{im} \tag{48}$$

Pre- and post-multiplying (18) with Φ_1, Φ_2 and their transposes, successively, combining (47) and (48), it can be inferred that (44) is an equivalent condition of (18). Moreover, from the definitions of the matrices related, we can notice that (45) and (46) are sufficient conditions to guarantee (19) and (20). The proof is completed. \square

Remark 9: In Theorem 2, there exist complex association relationships among the relevant scalars and matrices. However, by prescribing $\delta_m, \alpha_m, \mu_m, \vartheta, D_{\min}, D_{\max}, \tau_a, \tau_b, \rho_{iml}$ and h in advance, the inequalities (44)–(46) are integrated into linear matrix inequations (LMIs). Through the LMI Toolbox in MATLAB, we

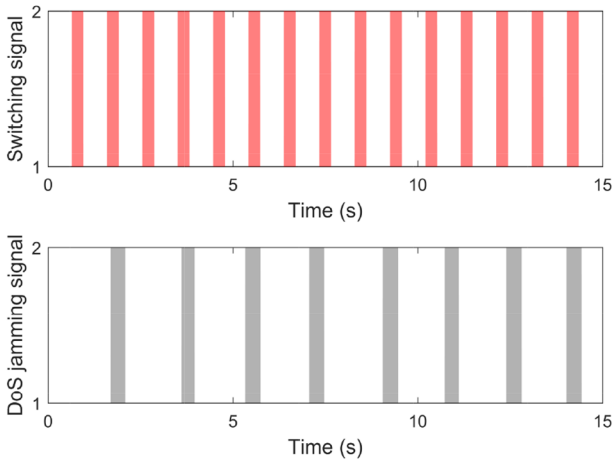


Fig. 4 Switching signal and DoS jamming signal

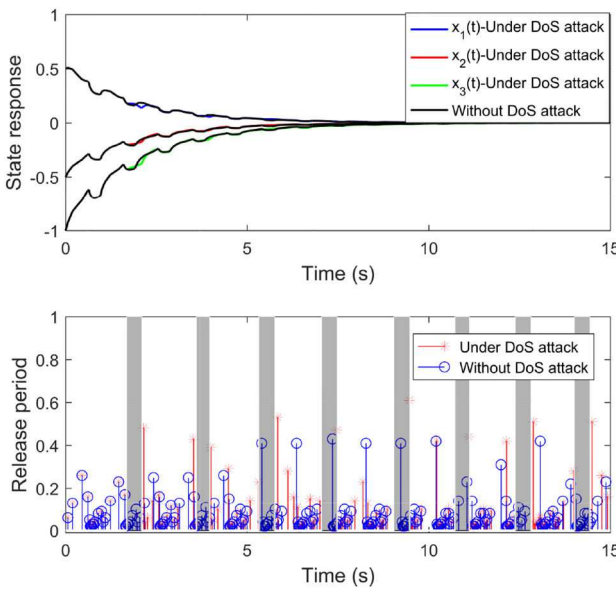


Fig. 5 State responses and release period

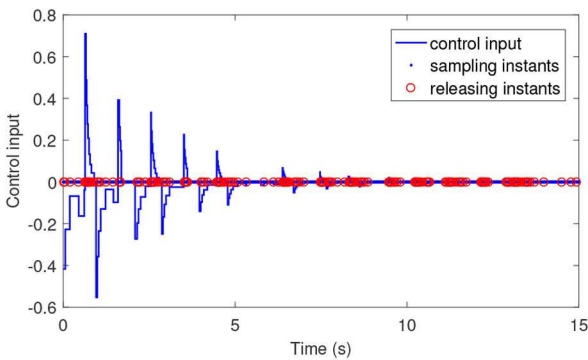


Fig. 6 Response of the control input

first gain the matrices Y_{im} , X_{im} and $\tilde{\Omega}_{im}$. Then, we can obtain the event-triggered parameters $\Omega_{im} = X_{im}^{-1} \tilde{\Omega}_{im} X_{im}^{-1}$ and the switching controller gains $K_{im} = Y_{im} X_{im}^{-1}$.

4 Illustrative examples

In this section, the proposed approach will be verified by two illustrative examples.

Example 1: Consider the switched linear system [40] with

$$A_1 = \begin{bmatrix} -0.2274 & -0.0594 & 0.53 \\ -0.2667 & -0.883 & 0.081 \\ 0.133 & -0.74 & 0.1 \end{bmatrix}, \quad B_1 = \begin{bmatrix} -1.8555 \\ -1.204 \\ -2.2 \end{bmatrix}$$

$$A_2 = \begin{bmatrix} -0.1135 & 0.3756 & -0.21 \\ 0.6404 & -0.2835 & 0.33 \\ 0.1 & -0.344 & -0.1 \end{bmatrix}, \quad B_2 = \begin{bmatrix} -1.8555 \\ -1.204 \\ -2.2 \end{bmatrix}$$

By checking the eigenvalues of system matrices, it is clear that the original system is unstable without appropriate control input. The sampling period is set as $h = 0.01$, and we consider a non-periodic DoS attack signal $\Gamma(t)$ in (2) with power-constrained parameters $d_{\min} = 2$, $d_{\max} = 0.42$, $\tau_b = 2.01$, which yields $D_{\min} = 2$ and $D_{\max} = 0.43$ according to (9). Choosing $\alpha_1 = 0.32$, $\alpha_2 = 0.9$, $\mu_1 = 1.05$, $\mu_2 = 1.05$, $\vartheta = 1.1$ and $\tau_a = 0.4$ satisfies (17). Let $\delta_1 = 0.2$, $\delta_2 = 100$, $\rho_{iml} = 1.5$, $i \in \{1, 2\}$, $m \in \{1, 2\}$ and $l \in \{1, 2\}$. It is worth pointing out that $\delta_2 = 100$ is large enough to guarantee no events triggered compared to $\delta_1 = 0.2$, which effectively simulates the influences of DoS attacks. By solving the matrix inequalities in Theorem 2, the weighting matrices Ω_{11} and Ω_{21} of the online event trigger and the switching controller gains K_{im} are given as follows:

$$\Omega_{11} = \begin{bmatrix} 20.64 & -1.458 & 12.38 \\ -1.457 & 0.6850 & -1.403 \\ 12.38 & -1.403 & 8.364 \end{bmatrix}, \quad (49)$$

$$\Omega_{21} = \begin{bmatrix} 28.09 & 25.10 & -1.344 \\ 25.10 & 23.17 & -1.723 \\ -1.344 & -1.723 & 0.4415 \end{bmatrix}$$

$$\begin{cases} K_{11} = [3.361 & -0.4740 & 2.334] \\ K_{12} = [0.0017 & 0.0003 & 0.0008] \\ K_{21} = [4.455 & 4.185 & -0.3594] \\ K_{22} = [0.4968 & 0.3108 & 0.0662] \end{cases} \quad (50)$$

For simulation, we set the initial state as $x_0 = [0.5 \quad -0.5 \quad -1]^T$. A non-periodic DoS attack signal is produced randomly according to the prescribed power-constrained parameters as shown in Fig. 4. The switching signal satisfying $\tau_a = 0.4$ is also depicted in Fig. 4, in which at most 37 switchings are permitted over $[0, 15]$ s. It can be found that the DoS attack sequence, the switching sequence and the sampling sequence are interlaced, which reveals the essential reason for the complexity of time series analysis in this work. Fig. 5 shows the responses of system state and the corresponding release period over $[0, 15]$ s. It is indicated that the switched system is asymptotic stable with and without DoS attacks. Owing to the switching controllers K_{12} and K_{22} , roughly identical control performance can be gained in the two situations. It indeed saves network resources, that is, only 185 sampled data are transmitted while the total sampled data comes to 1500 over $[0, 15]$ s. Moreover, it is demonstrated that no data can be successfully transmitted during the active interval of DoS attacks. Fig. 6 illustrates the response of the control signal, whose every jump is corresponding to a process of system switching, event triggering or controller switching due to DoS attacks.

Example 2: A second-order oscillating circuit [41] as shown in Fig. 7 is introduced as a practical engineering example to further manifest the feasibility and effectiveness of the proposed theories, which can be modelled with two switching modes (S_1, S_2). In the framework, R_0, R_1, R_2, R_3 denote the linear resistance, C represents the capacitor, the current source $G(V_C) = -aV_C$, and E_v denotes the remote-controlled input voltage to guarantee the circuit system stable. By normalisation methods as in [41], its state equations can be expressed by (Fig. 8)

$$\begin{cases} \dot{X} = A_1 X + B_1 u & \text{when } S_1 \text{ is on} \\ \dot{X} = A_2 X + B_2 u & \text{when } S_2 \text{ is on} \end{cases} \quad (51)$$

where

$$X = \begin{bmatrix} x_1 \\ x_2 \end{bmatrix},$$

$$x_1 = \sqrt{L}i_L, x_2 = \sqrt{C}V_C, \dot{X} = dX/d\tau, \tau = t/\sqrt{LC},$$

$$A_1 = \begin{bmatrix} -\kappa & -1 \\ 1 & 1-g_1 \end{bmatrix}, A_2 = \begin{bmatrix} -\kappa & -1 \\ 1 & 1-g_2 \end{bmatrix}, B_1 = \begin{bmatrix} 0 \\ b_1 \end{bmatrix}, B_2 = \begin{bmatrix} 0 \\ b_2 \end{bmatrix}$$

$$u = E_v, \quad \kappa = R_3\sqrt{C/L}, \quad g_1 = 1 - (a - (1/(R_0 + R_1)))\sqrt{L/C},$$

$$b_1 = \sqrt{L}/(R_0 + R_1), \quad g_2 = 1 - (a - (1/(R_0 + R_2)))\sqrt{L/C} \quad \text{and}$$

$$b_2 = \sqrt{L}/(R_0 + R_2).$$

Choosing $\kappa = 0.6$, $g_1 = 0.1$, $g_2 = 10$, $b_1 = 0.1$, $b_2 = 5$, we can notice that the circuit system is unstable without appropriate input voltage. Moreover, a non-periodic DoS attack signal $\Gamma(t)$ in (2) is considered as shown in Fig. 8. As in Example 1, the related parameters are given as: $d_{\min} = 1.1$, $d_{\max} = 0.7$, $\tau_a = 0.4$, $\tau_b = 1.11$, $\alpha_1 = 1$, $\alpha_2 = 1.25$, $\mu_1 = 1.03$, $\mu_2 = 1.05$, $\vartheta = 1.05$, $\delta_1 = 0.3$, $\delta_2 = 100$, $\rho_{iml} = 1.6$, $i \in \{1, 2\}$, $m \in \{1, 2\}$ and $l \in \{1, 2\}$. Then, the corresponding weighting matrices of the online event trigger and the switching controller gains K_{im} are given as follows:

$$\Omega_{11} = \begin{bmatrix} 0.8010 & -2.046 \\ -2.046 & 5.276 \end{bmatrix}, \quad \Omega_{21} = \begin{bmatrix} 0.8732 & -1.124 \\ -1.124 & 1.644 \end{bmatrix} \quad (52)$$

$$\begin{cases} K_{11} = [22.81 & -59.07] \\ K_{12} = [0.0016 & -0.0012] \\ K_{21} = [0.3561 & -0.4729] \\ K_{22} = [0.0017 & -0.0016] \end{cases} \quad (53)$$

Simulation results are demonstrated in Figs. 9 and 10. In summary, it comes to a similar conclusion as Example 1, which shows huge potential of the proposed algorithm in the active control of circuit systems.

In addition, for this example, the relationships of various parameters are investigated. From (17), we can notice that there is a restrictive relationship between the power-constrained parameters, d_{\min} and d_{\max} . Meanwhile, the power-constrained parameters should have effects on the decay rate ρ to the point of theoretical analysis. During the analysis, the prescribed system parameters above is used as a set of reference parameters, and it is worth minding that we keep the remaining ones constant when discussing the relationship of two assigned parameters.

By a basic optimisation algorithm, the relationships are depicted in Tables 1–4. From Table 1, it is indicated that a larger active interval of DoS attacks is allowed with the increase of the sleeping interval. It is relatively consistent with the reality because a larger sleeping interval provides more control to counteract the negative effects caused by DoS attacks. Tables 2 and 3 are used to display the variation tendency of the decay rate ρ with the variation of d_{\min} and d_{\max} . We can notice that a larger active interval of DoS attacks slows down the rate of convergence while the larger the sleeping interval, the larger the decay rate. Moreover, the release number N_r for different values of δ_i is listed in Table 4. It can be inferred that δ_i has remarkable influence on the release number as well as the control performance.

5 Conclusion

This paper has investigated the event-based control issue of networked switched systems under non-periodic DoS attacks. With the cooperation of specific designs in the physical plant, a novel event-based communication scheme with a switching control strategy is developed, which is resilient to DoS attacks. By constructing a piecewise Lyapunov function, sufficient conditions

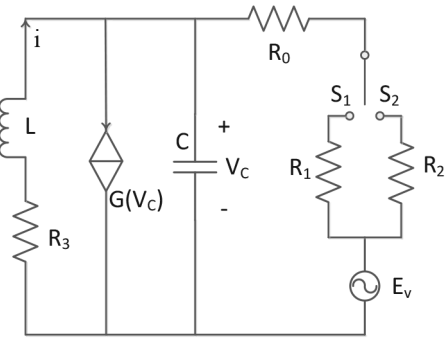


Fig. 7 Second-order oscillating circuit

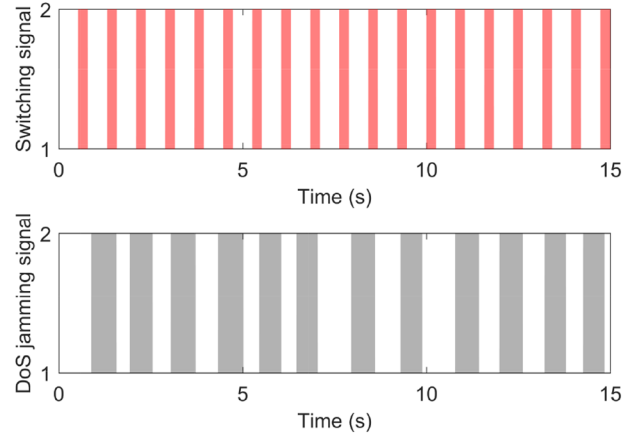


Fig. 8 Switching signal and DoS jamming signal

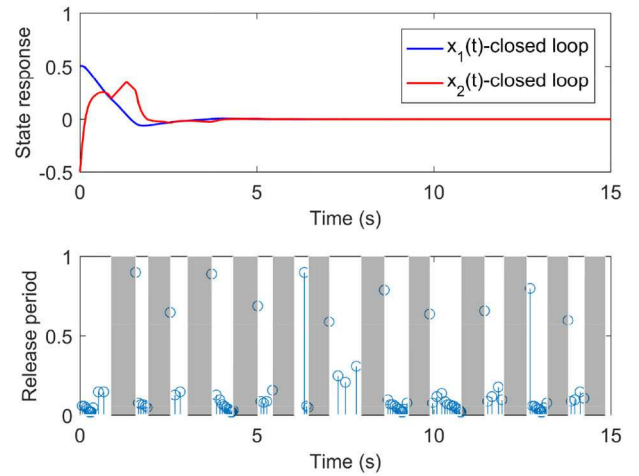


Fig. 9 State responses and release period

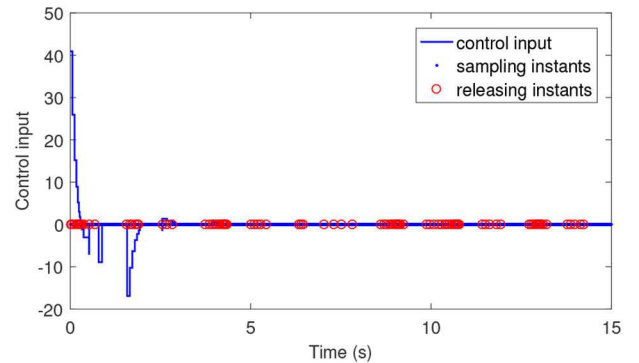


Fig. 10 Response of the control input

for exponential stability are obtained. Switching controller gains and event-triggering parameters can be designed based on the power constraints of DoS attacks. A numerical example is

Table 1 d_{\max} for different values of d_{\min}

d_{\min}	0.5	1	3	5	7
d_{\max}	0.32	0.7	2.2	3.7	5.2

Table 2 ρ for different values of d_{\max}

d_{\max}	0.1	0.3	0.5	0.6	0.7
ρ	0.7443	0.4968	0.2492	0.1255	0.0015

Table 3 ρ for different values of d_{\min}

d_{\min}	1	3	5	6	7
ρ	0.0015	0.6245	0.7501	0.7815	0.8040

Table 4 Releasing number N_r for different values of δ_1 over [0, 15 s]

δ_1	0.05	0.1	0.3	0.5	0.7
N_r	194	164	124	110	102

illustrated to verify the proposed method. Moreover, the method is successfully applied to the active control of a second-order oscillating circuit. The simulation results demonstrate the detailed relationships among exponential decay rate, event-triggering parameters and constraints of DoS attacks, which can further contribute to improving the control performance in practical applications.

6 Acknowledgments

This work was supported by a grant from the National Natural Science Foundation of China No. 61473156.

7 References

- [1] Zhu, K., Ma, D., Zhao, J.: 'Event triggered control for a switched lpv system with applications to aircraft engines', *IET Control Theory Appl.*, 2018, **12**, (10), pp. 1505–1514
- [2] Liberzon, D., Hespanha, J.P., Morse, A.S.: 'Stability of switched systems: a lie-algebraic condition', *Syst. Control Lett.*, 1999, **37**, (3), pp. 117–122
- [3] Cetinkaya, A., Ishii, H., Hayakawa, T.: 'Analysis of stochastic switched systems with application to networked control under jamming attacks', *IEEE Trans. Autom. Control*, 2019, **64**, (5), pp. 2013–2028
- [4] Zhang, H., Xie, D., Zhang, H., *et al.*: 'Stability analysis for discrete-time switched systems with unstable subsystems by a mode-dependent average dwell time approach', *ISA Trans.*, 2014, **53**, (4), pp. 1081–1086
- [5] Du, S., Karimi, H.R., Qiao, J., *et al.*: 'Stability analysis for a class of discrete-time switched systems with partial unstable subsystems', *IEEE Trans. Circuits Syst. II: Express Briefs*, 2019, **66**, (12), pp. 2017–2021
- [6] Zhang, M., Zhu, Q.: 'Input-to-state stability for non-linear switched stochastic delayed systems with asynchronous switching', *IET Control Theory Appl.*, 2019, **13**, (3), pp. 351–359
- [7] Zhang, D., Xu, Z., Karimi, H.R., *et al.*: 'Distributed filtering for switched linear systems with sensor networks in presence of packet dropouts and quantization', *IEEE Trans. Circuits Syst. I: Reg. Pap.*, 2017, **64**, (10), pp. 2783–2796
- [8] Xiao, X., Park, J.H., Zhou, L., *et al.*: 'Event-triggered control of discrete-time switched linear systems with network transmission delays', *Automatica*, 2020, **111**, pp. 1–6, doi: 10.1016/j.automatica.2019.108585
- [9] Gao, M., Hu, J., Chen, D., *et al.*: 'Resilient state estimation for time-varying uncertain dynamical networks with data packet dropouts and switching topology: an event-triggered method', *IET Control Theory Appl.*, 2020, **14**, (3), pp. 367–377
- [10] Li, M., Chen, Y.: 'Challenging research for networked control systems: a survey', *Trans. Inst. Meas. Control*, 2019, **41**, (9), pp. 2400–2418
- [11] Ding, T., Ge, M., Liu, Z., *et al.*: 'Discrete-communication-based bipartite tracking of networked robotic systems via hierarchical hybrid control', *IEEE Trans. Circuits Syst. I: Reg. Pap.*, 2020, **67**, (4), pp. 1402–1412, doi: 10.1109/TCSI.2019.2961804
- [12] Tabuada, P.: 'Event-triggered real-time scheduling of stabilizing control tasks', *IEEE Trans. Autom. Control*, 2007, **52**, (9), pp. 1680–1685
- [13] Yue, D., Tian, E., Han, Q.: 'A delay system method for designing event-triggered controllers of networked control systems', *IEEE Trans. Autom. Control*, 2013, **58**, (2), pp. 475–481

- [14] Tian, E., Wang, Z., Zou, L., *et al.*: 'Probabilistic-constrained filtering for a class of nonlinear systems with improved static event-triggered communication', *Int. J. Robust Nonlinear Control*, 2019, **29**, (5), pp. 1484–1498
- [15] Gu, Z., Shi, P., Yue, D., *et al.*: 'Decentralized adaptive event-triggered H_{∞} filtering for a class of networked nonlinear interconnected systems', *IEEE Trans. Cybern.*, 2019, **49**, (5), pp. 1570–1579
- [16] Liu, J., Wang, Y., Zha, L., *et al.*: 'Event-based control for networked T-S fuzzy cascade control systems with quantization and cyber attacks', *J. Franklin Inst.*, 2019, **356**, (16), pp. 9451–9473
- [17] Gu, Z., Zhang, T., Yang, F., *et al.*: 'A novel event-triggered mechanism for networked cascade control system with stochastic nonlinearities and actuator failures', *J. Franklin Inst.*, 2019, **356**, (4), pp. 1955–1974
- [18] Yan, S., Nguang, S.K., Shen, M., *et al.*: 'Event-triggered H_{∞} control of networked control systems with distributed transmission delay', *IEEE Trans. Autom. Control*, 2020, **65**, (10), pp. 4295–4301, doi: 10.1109/TAC.2019.2953460
- [19] Peng, C., Zhang, J., Han, Q.: 'Consensus of multiagent systems with nonlinear dynamics using an integrated sampled-data-based event-triggered communication scheme', *IEEE Trans. Syst. Man Cybern.: Syst.*, 2019, **49**, (3), pp. 589–599
- [20] Song, G., Mao, X., Li, T.: 'Robust quantised control of hybrid stochastic systems based on discrete-time state and mode observations', *Int. J. Control*, 2019, **92**, (8), pp. 1836–1845
- [21] Xiang, W., Johnson, T.T.: 'Event-triggered control for continuous-time switched linear systems', *IET Control Theory Appl.*, 2017, **11**, (11), pp. 1694–1703
- [22] Qi, Y., Liu, Y., Zhang, Q.: 'Dynamic output feedback \mathcal{L}_{∞} control for network-based switched linear systems with performance dependent event-triggering strategies', *IET Control Theory Appl.*, 2019, **13**, (9), pp. 1258–1270
- [23] Ren, H., Zong, G., Li, T.: 'Event-triggered finite-time control for networked switched linear systems with asynchronous switching', *IEEE Trans. Syst. Man Cybern.: Syst.*, 2018, **48**, (11), pp. 1874–1884
- [24] Yan, S., Nguang, S.K., Zhang, L.: 'Nonfragile integral-based event-triggered control of uncertain cyber-physical systems under cyber-attacks', *Complexity*, 2019, **2019**, pp. 1–14, doi: 10.1155/2019/8194606
- [25] Hu, Z., Liu, S., Yang, L., *et al.*: 'Distributed fuzzy filtering for load frequency control of non-linear interconnected power systems under cyber-physical attacks', *IET Control Theory Appl.*, 2020, **14**, (4), pp. 527–538
- [26] Shoukry, Y., Tabuada, P.: 'Event-triggered state observers for sparse sensor noise/attacks', *IEEE Trans. Autom. Control*, 2016, **61**, (8), pp. 2079–2091
- [27] Amin, S., Schwartz, G.A., Shankar Sastry, S.: 'Security of interdependent and identical networked control systems', *Automatica*, 2013, **49**, (1), pp. 186–192
- [28] Befekadu, G.K., Gupta, V., Antsaklis, P.J.: 'Risk-sensitive control under markov modulated denial-of-service (dos) attack strategies', *IEEE Trans. Autom. Control*, 2015, **60**, (12), pp. 3299–3304
- [29] De Persis, C., Tesi, P.: 'Input-to-state stabilizing control under denial-of-service', *IEEE Trans. Autom. Control*, 2015, **60**, (11), pp. 2930–2944
- [30] Ding, D., Han, Q.L., Xiang, Y., *et al.*: 'A survey on security control and attack detection for industrial cyber-physical systems', *Neurocomputing*, 2018, **275**, pp. 1674–1683
- [31] Sun, Y.C., Yang, G.H.: 'Event-triggered resilient control for cyber-physical systems under asynchronous dos attacks', *Inf. Sci.*, 2018, **465**, pp. 340–352
- [32] Zhang, Z.H., Liu, D., Deng, C., *et al.*: 'A dynamic event-triggered resilient control approach to cyber-physical systems under asynchronous dos attacks', *Inf. Sci.*, 2020, **519**, pp. 260–272
- [33] Sun, H., Peng, C., Zhang, W., *et al.*: 'Security-based resilient event-triggered control of networked control systems under denial of service attacks', *J. Franklin Inst.*, 2019, **356**, (17), pp. 10277–10295
- [34] Sun, Y.C., Yang, G.H.: 'Periodic event-triggered resilient control for cyber-physical systems under denial-of-service attacks', *J. Franklin Inst.*, 2018, **355**, (13), pp. 5613–5631
- [35] Hu, S., Yue, D., Xie, X., *et al.*: 'Resilient event-triggered controller synthesis of networked control systems under periodic dos jamming attacks', *IEEE Trans. Cybern.*, 2019, **49**, (12), pp. 4271–4281
- [36] Cheng, Z., Yue, D., Hu, S., *et al.*: 'Detection-based weighted H_{∞} LFC for multi-area power systems under dos attacks', *IET Control Theory Appl.*, 2019, **13**, (12), pp. 1909–1919
- [37] Liu, J., Gu, Y., Zha, L., *et al.*: 'Event-triggered h load frequency control for multiarea power systems under hybrid cyber attacks', *IEEE Trans. Syst. Man Cybern.: Syst.*, 2019, **49**, (8), pp. 1665–1678
- [38] Xu, Y., Fang, M., Wu, Z.G., *et al.*: 'Input-based event-triggering consensus of multiagent systems under denial-of-service attacks', *IEEE Trans. Syst. Man Cybern.: Syst.*, 2020, **50**, (4), pp. 1455–1464
- [39] Foroush, H.S., Martinez, S.: 'On triggering control of single-input linear systems under pulse-width modulated dos signals', *SIAM J. Control Optim.*, 2016, **54**, (6), pp. 3084–3105
- [40] Jiang, Z., Yan, P.: 'Asynchronous switching control for continuous-time switched linear systems with output-feedback', *Int. J. Control. Autom. Syst.*, 2018, **16**, (5), pp. 2082–2092
- [41] Zhao, Y., Feng, J., Tse, C.K.: 'Discrete-time modeling and stability analysis of periodic orbits with sliding for switched linear systems', *IEEE Trans. Circuits Syst. I Reg. Pap.*, 2010, **57**, (11), pp. 2948–2955